Analysis of the Effects of Lead Configuration on Cardiac Spectrum

Ferney Beltrán-Molina[1], Jesús Requena-Carrión[1], Juho Väisänen[2,3]

[1]University Rey Juan Carlos, Fuenlabrada, Madrid, Spain
[2]Department of Biomedical Engineering, Tampere University of Technology, Tampere, Finland
[3]BioMediTech, Tampere, Finland

Abstract

Dominant frequency (DF) mapping is a promising technique in the diagnosis and management of atrial fibrillation (AF). Two intracardiac DF mapping approaches have been developed based respectively on contact and noncontact leads, but the relationship between their DF values is not fully understood. Theoretically, the spectrum of cardiac signals from different leads can be different, and therefore their DF values could also be different. In this study we investigate the effects of lead configuration on the spectrum of cardiac signals. Signals measured by unipolar and bipolar lead systems are synthesized in a simulation environment, and their full spectra, bandwidth (BW) and DF values are analyzed. Our results suggest that the spectral BW and the lead spatial resolution are inversely related. By contrast, DF values are not affected by the lead configuration. We conclude that the DF is a robust spectral feature, whereas other spectral features depending on the BW can be distorted by the lead configuration.

1. Introduction

Cardiac fibrillation is a complex arrhythmia whose mechanisms of initiation and maintenance remain to date poorly understood. Traditionally, cardiac fibrillation has been described as a random and disorganized rhythm, in which different regions of the myocardium activate asynchronously at a high rate. However, the application of high resolution electrical and optical mapping techniques to the analysis of both atrial and ventricular fibrillation (AF and VF, respectively) suggests that cardiac fibrillation can have some degree of spatiotemporal organization [1].

During AF, the combination of high resolution mapping techniques with dominant frequency (DF) analysis, known as DF mapping, has revealed consistent spatiotemporal regularities in the myocardium, both in animal and in patient studies [2]. The observation of localized sources of high frequency activity in DF maps during paroxysmal AF has suggested that these sources may be actively involved in the initiation and maintenance of AF in humans. This mechanistic insight provided by DF mapping during AF, has led to the application of this technique as a guide for AF catheter based ablation [3], and its clinical potential is widely acknowledged.

Two intracardiac mapping systems have been used to construct DF maps in patients undergoing AF. Contact mapping systems such as CARTO (Biosense Webster Inc), sequentially measure local, bipolar electrogram signals from which DF values are extracted. Noncontact mapping systems such as EnSite (St. Jude Medical Inc) measure simultaneously global, unipolar electrogram signals from multiple electrodes, and then by using inverse methods reconstruct the activity of the atria, from which the DF is extracted. However, it has been shown for idealized leads that lead configuration can affect the spectrum of cardiac signals and specifically that the lead spatial resolution (SR) can affect the spectral envelope [4, 5]. Qualitatively similar effects could be expected for realistic leads, and thus there is the possibility that different leads provide different spectra and DF values for the same underlying AF episode.

In this study, we investigate the effects of lead configuration on the spectrum of cardiac signals. Two families of unipolar and bipolar signals are synthesized in a simulation environment, and their bandwidth (BW) and DF are analyzed. The relationship between the BW and the DF values and the lead SR are further explored.

2. Methods

In a simulation environment, we firstly simulate the activity of a $W \times W$ square sample of cardiac tissue. Secondly, the measurement sensitivity distribution of two families of unipolar and bipolar electrodes located at different heights h over the tissue sample are obtained, and their SR is computed. Then, the signals induced at each electrode by the activity of the tissue sample are synthesized. Finally, the power spectrum of each cardiac signal is estimated and their BW and DF are extracted. We use the BW and the DF to investigate the effects of lead configuration on the spectrum of cardiac signals.

2.1. Bioelectric model

We follow a lead-field approach to model cardiac signals [6]. According to lead-field theory, the cardiac signal $c(t)$ induced by a cardiac volume source V can be expressed as

$$c(t) = \int_V \mathbf{L}(v) \cdot \mathbf{J}(v,t) dv, \quad (1)$$

where $\mathbf{L}(v)$ is the measurement sensitivity distribution of the lead system, $\mathbf{J}(v,t)$ is the time-varying distribution of cardiac dipoles in the volume source V, and $(\cdot)$ denotes dot product. In words, cardiac signals are a linear combination of the cardiac dipoles, and the lead measurement distribution describes the ability of the lead system to measure each cardiac dipole. Based on the measurement sensitivity distribution, we also define its normalized magnitude $L(v) = \|\mathbf{L}(v)\| / \max\{\|\mathbf{L}(v)\|\}$.

2.1.1. Lead models

We use two families of unipolar and bipolar electrodes. Let $v_0 \notin V$ denote the point of the space where the electrode is located, and $D(v, v_0)$ denote the distance between a point within the volume source, $v \in V$ and v_0. Following [7], the measurement sensitivity distributions $\mathbf{L}_u(v)$ and $\mathbf{L}_b(v)$ of respectively a unipolar and a bipolar electrode located at v_0 are defined as

$$\mathbf{L}_u(v) = \frac{1}{D(v,v_0)^2} \hat{r} \quad (2)$$

$$\mathbf{L}_b(v) = \frac{1}{D(v,v_0)^3} \hat{r}, \quad (3)$$

where $\hat{r}$ is a unitary radial vector connecting v to v_0. We locate v_0 at the center of the tissue sample and at different heights h, where $0 < h/W < 0.2$.

2.1.2. Lead spatial resolution

We measure the SR of a lead by using on the notion of Lead Equivalent Volume (LEV). The LEV is analogous to the notion of beam solid angle in antenna theory, which describes the ability of an antenna to concentrate radiated power in a given direction [8]. Based on the normalized lead sensitivity distribution $L(v)$, the LEV is defined as

$$\text{LEV} = \int_V L_n(v) dv. \quad (4)$$

The LEV quantifies the size of the region within the volume source where leads concentrate their measurement, and can take the values $0 < \text{LEV} < 1$. Based on the LEV, the lead SR is defined as the inverse of the LEV, $\text{SR} = 1/\text{LEV}$. Thus, $1 < \text{SR} < \infty$.

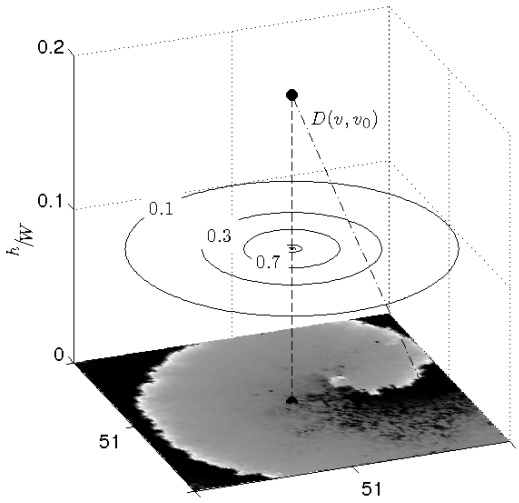

Figure 1. Simulated spiral wave on a 101×101 square sample of cardiac tissue. Electrodes are located over the center of the tissue sample and their sensitivity is defined in terms of the distance $D(v, v_0)$.

2.2. Cardiac dynamics model

We model cardiac dynamics by following a cellular automata approach previously proposed in [9]. This model of cardiac dynamics is simple and has a low computational burden. Furthermore, it is able simulate complex cardiac spatiotemporal dynamics, such as fibrillatory conduction and spiral waves. Based on this model, we simulated two spatiotemporal activation patterns of duration 20 s, in a square sample of cardiac tissue consisting of 101×101 discrete elements, i.e. $W = 101$. The first activation pattern consists of a train of plane waves traveling on the x-direction at a rate of 1 Hz. The second activation pattern consists of a spiral rotating around the center of the tissue sample at a rate of approximately 7 Hz (Figure 1). We use simulated activations to generate a time-varying distribution of dipoles which in combination with the lead sensitivity distributions, allow us to synthesize cardiac signals. Finally, cardiac signals are sampled at 500 Hz.

2.3. Spectrum estimation

The power spectrum of synthesized cardiac signals is estimated by using Welch's method. A Hamming window of 2048 samples and 50% overlap is used for achieving a high resolution in frequency in the estimation of the power spectrum. Based on the estimated power spectrum, the 90% power BW is computed for each signal and the DF is visually identified as the frequency separation between consecutive harmonics.

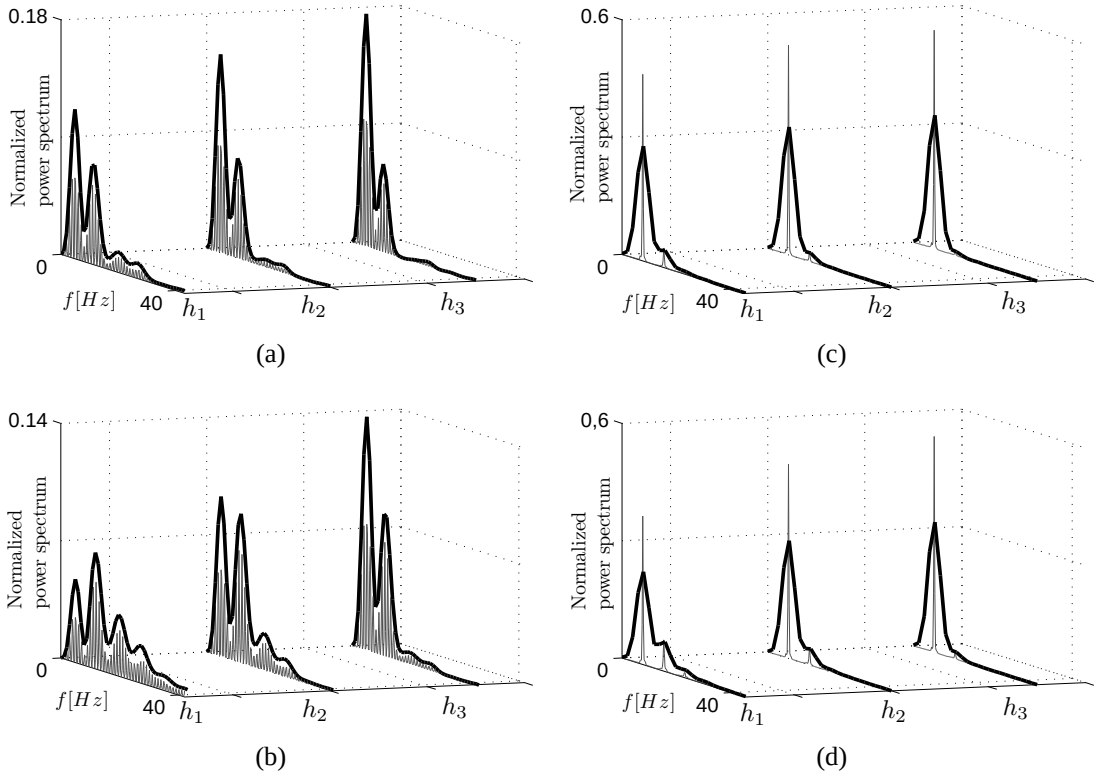

Figure 2. Spectrum of cardiac signals synthesized from unipolar and bipolar electrodes during plane-wave and spiral spatiotemporal dynamics, for electrodes located at heights $h_1/W = 0.09$, $h_2/W = 0.14$ and $h_3/W = 0.2$. (a) Unipolar electrode, plane-wave; (b) bipolar electrode, plane-wave; (c) unipolar electrode, spiral; (d) bipolar electrode, spiral.

Table 1. BW of signals from unipolar and bipolar electrodes located at h_1, h_2 and h_3, during plane-wave (P) and spiral (S) dynamics.

Distance	BW$_u$ (P)	BW$_b$ (P)	BW$_u$ (S)	BW$_b$ (S)
h_1	23.2	33.2	15.1	20.5
h_2	13.9	22.0	8.1	15.1
h_3	12	13.9	7.8	7.8

Table 2. SR of unipolar and bipolar electrodes located at h_1, h_2 and h_3, during plane-wave (P) and spiral (S) dynamics.

Distance	SR$_u$	SR$_b$
h_1	5.0	10.3
h_2	2.8	4.9
h_3	1.9	2.9

3. Results

Spectra from synthesized cardiac signals show a quasi-periodic structure consisting of harmonic frequencies (Fig. 2). Irrespective of the electrode configuration, the separation between harmonic frequencies, which we took as the DF, is 1 Hz during plane-wave dynamics and 7 Hz during spiral dynamics. This observation is consistent with the simulated spatiotemporal dynamics. By contrast, the distribution of power among harmonic frequencies depends on the electrode configuration. Figure 2 and Table 1 show the spectrum and the BW of cardiac signals for electrodes located at $h_1/W = 0.09$, $h_2/W = 0.14$ and $h_3/W = 0.2$, during plane-wave and spiral dynamics. Unipolar electrodes have a narrower BW than bipolar ones and also, the higher h, the narrower the BW. This can also be concluded from Figure 3, which shows the relationship between the BW and the electrode height h for $0 < h/W < 0.2$.

Our results indicate that irrespective of the electrode configuration, the relationship between BW and lead SR is approximately fixed, and that the larger the LEV (the lower the SR) the narrower the BW (Figure 4). For illustrative purposes, Table 2 shows the SR of unipolar and bipolar electrodes located at h_1, h_2 and h_3. The SR of bipolar electrodes at h_2 and h_3 is approximately the same as the SR of unipolar electrodes located respectively at h_1 and h_2. Table 1 shows that bipolar electrodes at h_2 and h_3 have the same BW as unipolar electrodes at h_1 and h_2.

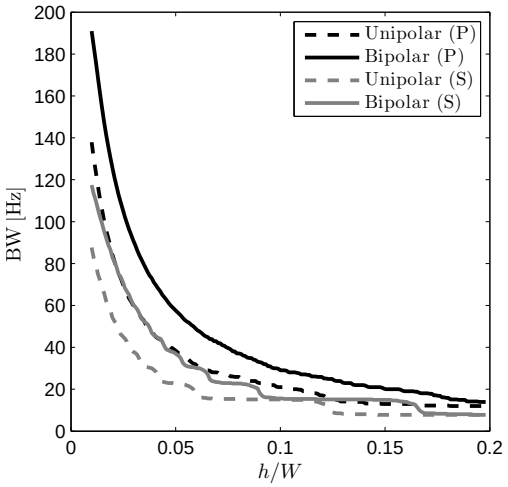

Figure 3. Relationship between BW and electrode height during plane-wave (P) and spiral (S) dynamics.

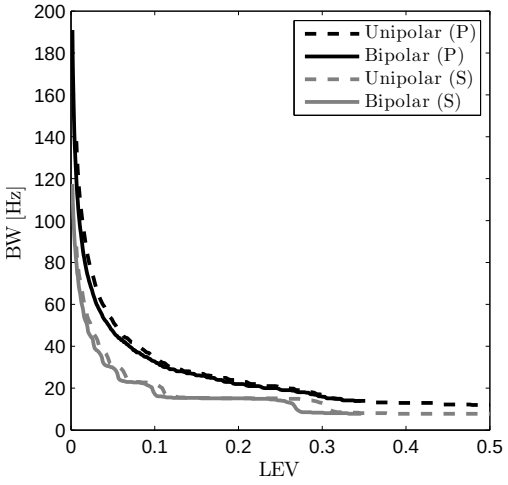

Figure 4. Relationship between BW and LEV during plane-wave (P) and spiral (S) dynamics.

4. Discussion and conclusions

We have explored in a simulation environment the effects of lead configuration (electrode type and height) on the spectrum of cardiac signals. Our results show that the DF is not affected by the lead configuration. By contrast, lead configuration affects the spectral BW. In general, unipolar electrodes have a narrower BW than bipolar electrodes and the further away the electrode is from the cardiac source, the narrower the BW. Our results also suggest that irrespective of the lead configuration the relationship between BW and lead SR is fixed. In other words, two leads that have similar SR will measure signals of similar BW. This effect has been previously proved for idealized leads [4], but to the best of our knowledge it has not been described for arbitrary leads.

Our results have practical implications, since they indicate that DF maps may not be affected by the lead configuration. However, other spectral indices depending on the BW could be distorted by the lead system. Understanding the spectral effects of lead systems can contribute to elucidate how physiological information manifests in the spectrum of cardiac signals.

References

[1] Jalife J. Ventricular fibrillation: Mechanisms of initiation and maintenance. Annual Review of Physiology 2000;62(1):25–50.

[2] Berenfeld O. Toward discerning the mechanisms of atrial fibrillation from surface electrocardiogram and spectral analysis. Journal of Electrocardiology 2010;43(6):509–514.

[3] Atienza F, Almendral J, Moreno J, Vaidyanathan R, Talkachou A, Kalifa J, Arenal A, Villacastin JP, Torrecilla EG, Sanchez A, Ploutz-Snyder R, Jalife J, Berenfeld O. Activation of inward rectifier potassium channels accelerates atrial fibrillation in humans: evidence for a reentrant mechanism. Circulation 2006;114(23):2434–2442.

[4] Requena-Carrión J. Análisis espectral de electrogramas almacenados en desfibrilador automático implantable durante fibrilación ventricular, Ph.D. Dissertation. Spain: Universidad Carlos III de Madrid, 2008.

[5] Beltrán-Molina F, Muñoz-Gomez A, Rodríguez A, Vinagre J, Requena-Carrión J. Effects of lead spatial resolution on the spectrum of cardiac signals: A simulation study. In Engineering in Medicine and Biology Society, EMBC, 2011 Annual International Conference of the IEEE 2011;30(3): 3800 –3803.

[6] Malmivuo J, Plonsey R. Bioelectromagnetism: principles and applications of bioelectric and biomagnetic fields. New York: Oxford University Press, 1995.

[7] Jenkins JM. Impact of electrode placement and configuration on performance of morphological measures of intraventricular electrograms. In IEEE Computers in Cardiology 1992; 367–370.

[8] Balanis CA. Antenna theory: analysis and design. Hoboken New Jersey: John Wiley & Sons, 2005.

[9] Alonso-Atienza F, Requena-Carrión J, García-Alberola A, Rojo-Álvarez JL, Sánchez-Muñoz JJ, Martinez-Sánchez J, Valdés-Chávarri M. A probabilistic model of cardiac electrical activity based on a cellular automata system. Revista Española de Cardiología Jan 2005;58(1):41–47.

Address for correspondence:

Ferney A. Beltrán-Molina
University Rey Juan Carlos
Cmno del Molino s/n, Departamental III, D011
28943, Fuenlabrada, Madrid, Spain
ferney.beltran@urjc.es